The Frasnian–Famennian events in a deep-shelf succession, Subpolar Urals: biotic, depositional, and geochemical records

ALEXANDRA B. YUDINA, GRZEGORZ RACKI, NORMAN M. SAVAGE, MARIA RACKA, and KRZYSZTOF MAŁKOWSKI

Yudina, A.B., Racki, G., Savage, N.M., Racka, M., and Małkowski, K. 2002. The Frasnian–Famennian events in a deep-shelf succession, Subpolar Urals: biotic, depositional and geochemical records. *Acta Palaeontologica Polonica* 47 (2): 355–372.

The Frasnian–Famennian (F–F) boundary is well biostratigraphically documented in the *Palmatolepis*-rich deposits exposed along the Syv'yu River in the lower slopes of the Subpolar Urals. The thin-bedded calcareous-clayey-siliceous deep-slope succession of the Vorota Formation appears to represent continuous Domanic-type deposition throughout the world-wide carbonate crisis time, without evidence for the basal Famennian hiatus or a large-scale sedimentary perturbation within a regressive setting. The northernmost Laurussian sequence exhibits many well known signatures throughout the broad F–F timespan: the appearance of organic- and clay-rich deposits, icriodontid and radiolarian blooms, and a correlative shift of several geochemical proxies towards hypoxic and high-productivity regimes, perfectly recorded by positive $^{13}C_{carb}$ excursions of +3.5‰. Integrative biotic, microfacies and geochemical data substantiate a longer-term oceanographic destabilization, attributable to multiple Earth-bound triggering factors in (episodically enhanced?) greenhouse climate and punctuated eustatic sea-level highstands, superimposed on the elevated deposition of organic carbon-rich sediments during the Upper Kellwasser Event. Unsteady eutrophicated, and oxygen-depleted ecosystems during the F–F biotic crisis interval could be assumed, especially when intensified by various spasmodic tectono-volcanic phenomena in the incipiently closing Ural Ocean.

Key words: Frasnian; Famennian; Kellwasser Crisis; conodonts, microfacies, carbon isotopes; geochemistry; Timan-Pechora Basin.

Alexandra B. Yudina [alexa_geo@yahoo.com], Institut Geologii, Komi Nauchnyj Tsentr, Uralskoye Otdeleniye, Syktyvkar, Russia;
Grzegorz Racki [racki@us.edu.pl], Maria Racka [racka@ultra.cto.us.edu.pl], Wydział Nauk o Ziemi, Uniwersytet Śląski, ul. Będzińska 60, PL-41-200 Sosnowiec, Poland;
Norman M. Savage [nmsavage@oregon.uoregon.edu], Department of Geological Sciences, University of Oregon, Eugene, OR 97403, USA;
Krzysztof Małkowski [malk@twarda.pan.pl], Instytut Paleobiologii PAN, ul. Twarda 51/53, PL-02-089 Warszawa, Poland.

Introduction

The Devonian Frasnian–Famennian (F–F) biotic turning point is one of the most prominent extinction events during the Phanerozoic (see McGhee 1996 for general review). Different causal factors and feedbacks have been suggested to explain the biospheric perturbation, but especially a leading role of extraterrestrial impact(s) remains doubtful (McGhee 1996; Walliser 1996). Multicausal and exclusively Earth-bound trigger factors have recently received considerable attention, especially worldwide anoxic events and progressive cooling (see Copper 1998; Joachimski et al. 2002; Racki et al. 2002), and the general term "Kellwasser (KW) Crisis", merging both the late Frasnian anoxic pulses (Schindler 1993), is used here. Although there have already been many studies devoted to the F–F key interval, basic biotic, sedimentological, and geochemical data remain elusive or poorly known in many regions.

Unfortunately, the modern studies are limited to an equatorial belt, and high-resolution data from especially high northern latitudes are urgently required. In North Eurasia, such deep-water F–F sequences are accessible, as exemplified by the Kolyma River basin (Gagiev 1985, 1997; see also Karaulov and Gretschischnikova 1997). However, exclusively the more southward-located Timan-Pechora Basin, north-eastern East European Craton (recently Northwestern Russia; Fig. 1A), is well-known in the biostratigraphy and sequence stratigraphy contexts (Becker et al. 2000; House et al. 2000). This study is aimed to resolve the palaeoenvironmental evolution of the deep-shelf continuous sequence in the Subpolar Urals, Syv'yu river section (see Figs. 1–4), investigated previously in terms of conodont biostratigraphy

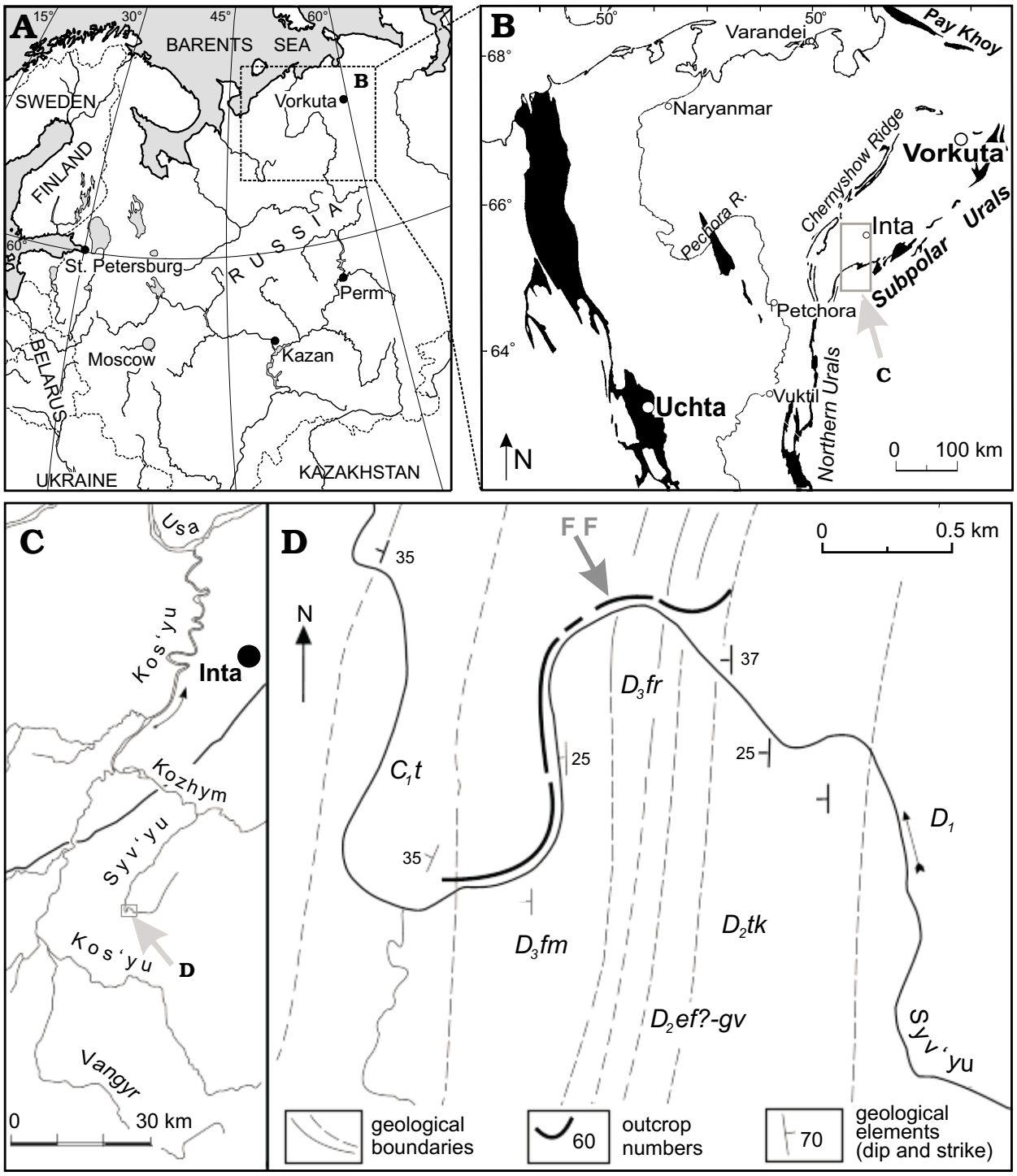

Fig. 1. Location of the studied area in Russia (**A**) and Timan-Pechora region (**B**, modified from Becker et al. 2000: fig. 1A), and location of the Kozhym River basin (**C**) and locality map of studied outcrops along the Syv'yu River section (**D**), western slopes of the Subpolar Urals; C_1t, Tournaisian. D_1, Lower Devonian; D_2tk, ?Middle Devonian, Takata Suite; D_2ef-gv, Eifelian–Givetian; D_3fr, Frasnian; D_3fm, Famennian.

(Savage and Yudina 1999, 2001). Refined integrative documentation of biostratigraphic, depositional and geochemical signatures across the critical stage boundary is provided for the first time for this part of Laurussian shelf, and the regional influence of anoxic events, eutrophication and volcanic phenomena is evaluated for the KW Crisis.

Materials and methods

The Upper Devonian outcrops along the Syv'yu River in the lower slopes of the Subpolar Urals were sampled extensively for conodont biostratigraphy, microfacies and geochemistry.

Fig. 2. F–F boundary beds exposed along the right bank of Syv'yu River, outcrop 2 (line marks F–F boundary; for location see Fig. 1D).

Ninety-nine samples were taken largely bed by bed, and studied in centimeter intervals around the F–F boundary. Sixty-eight thin sections were used in the petrological investigation.

Fifty-two whole rock, limestone to clayey shale samples from the 3.85 m thick interval were studied geochemically at the Activation Laboratories, Ontario, Canada (see Appendix 1 and 2). Fifty-four samples from a broader interval were investigated for carbon and oxygen isotopes at the Isotope Laboratory of Institute of Geological Sciences and Institute of Paleobiology, Polish Academy of Sciences in Warsaw. Major oxides and trace elements like Ba, Sr, V, Y, and Zr were determined by inductively coupled plasma atomic emission spectrometry (ICP-AES) following sample fusing with $LiBO_2$ and dissolving in HNO_3. The elements Ag, Cd, Cu, Ni, Pb, and Zn were also analyzed by ICP-AES but following sample digestion with HCl-HNO_3-$HClO_4$-HF. Analyses were carried out using two types of spectrometers: a Jarrell Ash model Enviro and a Perkin Elmer 6000. Precision and accuracy for the results were better than ±10% for concentrations at and higher than one hundred times the detection limit, ±15 20% for concentrations at and higher than ten times the detection limit, and ±100% on the level of the detection limit. Twenty one other elements (As, Au, Co, Cr, Cs, Hf, Ir, Mo, Rb, Sb, Sc,Th, U, La, Ce, Nd, Sm, Eu, Tb, Yb, and Lu) were measured by instrumental neutron activation analysis (INAA). The samples were irradiated in a thermal neutron flux of 5×10^{12} n cm^{-2} sec^{-1} and counted on two Ge crystal detectors Ortec and Canberra seven days after irradiation. Precision and accuracy for the results obtained by INAA method were better than ±5% for concentrations at and higher than one hundred times the detection limit, ±10 15% for concentrations at and higher than ten times the detection limit, and ± 100% on the level of the detection limit.

The carbon and oxygen isotopic analyses were carried out on CO_2 obtained by sample material reaction with 100% H_3PO_4 at 25°C for 24 hours. The measurements were made on a Finnigan MAT Delta plus mass-spectrometer equipped with Isodat 6.0 software. The results are expressed in ‰ relative to the PDB standard, using a NBS-19 reference sample. The accuracy of measurements approximates +0.02‰ for ^{13}C and +0.04‰ for ^{18}O.

Preliminary mineralogical analyses of acid-insoluble residues (IR) were performed at the Department of Earth Sciences, Silesian University, Poland. IR was obtained from reaction with 1N HCl for 24 hours at room temperature. Samples of IR were investigated for major mineralogical phases by X-ray diffraction (XRD) on a Philips PW 3710 diffractometer. Relative mineral abundances were determined semiquantitatively by using the ratios of the peak intensities of major minerals. In addition, the total organic carbon (TOC) content in four samples was determined using a non-automatic Leco CR-12 analyser.

Regional setting

The Timan-Pechora Basin is located in the north-east of the East European Craton. Structurally it is considered as the Pechora Plate, limited to the west by the East-Timan Thrust and to the east by the Main Urals Thrust (see Savage and Yudina 1999; House et al. 2000) The basin comprises an Upper Proterozoic basement overlain by Paleozoic–Cenozoic sedimentary cover. The basement consists of metamorphosed rocks represented by green schists, quarzites, sandstones, dolostones, limestones and intrusive rocks. Within the Timan Ridge and Urals, the rocks of the basement are exposed in the higher area, but on the platform they are buried to a significant depth and have been revealed only by deep drilling. The sedimentary cover consists of three structurally separated stratigraphic sequences: 1) Upper Cambrian–Lower Devonian, 2) Middle Devonian–Triassic (Lower Jurassic?), and 3) Middle Triassic–Recent. The thickness of cover changes from 4–7 km in the central part within the Pechora Syneclise to 10–14 km in the Pre-Urals foredeep. Within some of uplifts and domes the sedimentary thickness does not exceed 3–4 km, and on the Timan Ridge it is missing.

On the basis of discontinuities and unconformities, the widespread Middle Devonian–Triassic unit (see Fig. 1B) is subdivided into five subunits: Middle Devonian, Frasnian–Tournaisian, Visean–Lower Artinskian, Upper Artinskian–Upper Permian, and Triassic. The Frasnian–Tournaisian subunit consists of gray-colored sandstones, shales, and carbonates, 350–1400 m thick. The last are characterized by increasing compositional variability westward, caused by replacement of marine by lagoon-marine-continental conditions.

Upper Devonian Syv'yu River section

In the Late Devonian, the territory of the Pechora Plate was occupied by an epicontinental sea. In general, there are three

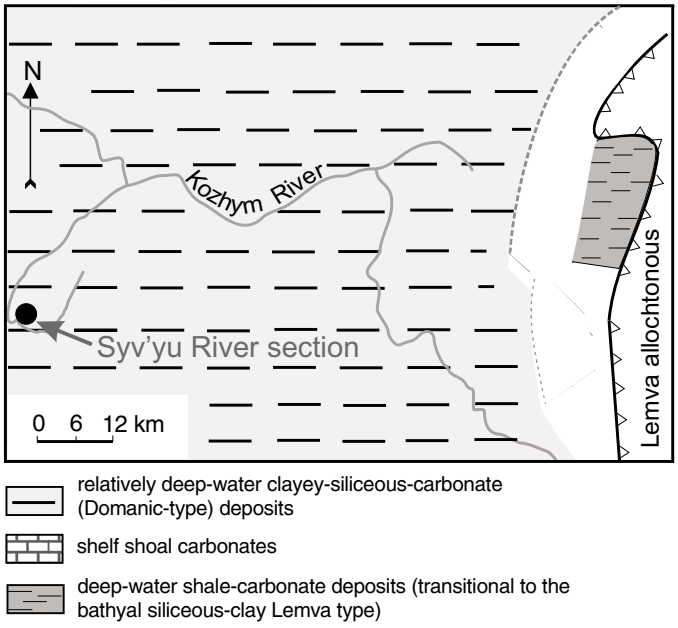

Fig. 3. Late Devonian facies distribution in the Kozhym River basin, western Subpolar Urals (based on Savage and Yudina 1999: fig. 3).

structural-facies complexes, corresponding to three zones of the Ural Ocean (see Yudin and Dedeev 1987; Yudin 1994): 1) shelf (inner shallow-water, middle, outer deep shelves), 2) continental slope, and 3) bathyal (so-called Lemva facies type of the starved Sakmarian back-arc basin; Ziegler 1988: 33; Khain and Seslavinsky 1996: 159, 185). The Late Devonian facies distribution was a result of the latest Givetian(?)–Frasnian onlap, drowning vast areas of the eastern margin of East European Craton that was caused by both tectonic activities and eustatic sea-level changes.

The Kozhym River basin under study (Fig. 1C, D) belongs to the West-Urals structural zone where Devonian deposits are widespread. The Upper Devonian deposits are represented by three facies types (Novakova 1991; see Fig. 3): 1) a Domanic-type, widespread in the western part of area, characterized by relatively deep-water bituminous sediments of a stagnant intra-shelf basin, with siliceous, terrigenous, and carbonate components, 2) a carbonate type, common in the eastern part of the area, represented by bioclastic, clotted, detrital, stromatoporoid-algal, and oncolitic limestones deposited within a shelf carbonate shoal, 3) relatively deep-water shale-carbonate deposits transitional to the siliceous-clay Lemva type that accumulated eastward from the carbonate shoal.

The Syv'yu River section is located about 38 km upstream from its junction with the Kozhym River. The Upper Devonian deposits, exposed along the right bank of Syv'yu River in several outcrops (Figs. 1D, 2), represent an almost continuous sequence of the Domanic facies type through the Frasnian and lower Famennian, and comprise thinly bedded, westerly dipping strata, without tectonic complications.

Previous works.—Modern stratigraphic studies of the Upper Devonian deposits in the Subpolar Urals stem from the work of Pershina (in Pershina et al. 1971), who subdivided the Frasnian succession into Pashiya, Kyn Horizons (Lower Frasnian), and Sargaevo, Domanic Horizons and Shar'yu Suite (Middle Frasnian), and Askyn, and Barma Horizons (Upper Frasnian). The Famennian was subdivided into Lower and Upper Famennian substages.

The Upper Devonian conodont faunas from the Syv'yu River succession were first studied by Deulin (1978). Later, in the course of large-scale mapping, the zonation established by this author was changed and correlated with regional horizons of the western Urals. In 1987 the Frasnian and Lower Famennian succession in the Syv'yu River section was measured by Yudina and Tsyganko (see Tsyganko 1994). Subsequently, during a field trip in August 1996, Yudina and Savage collected a rich fauna of conodonts in this section, and the F–F transition was exposed by digging a trench into the steep face of the river bank where the softer argillaceous strata had become weathered. Additional sampling for microfacies and geochemical purposes has been undertaken in 1999 (see Fig. 4). Some results of the conodont study have been published by Yudina (1989, 1994) and Savage and Yudina (1999, 2001).

Lithostratigraphy.—The total thickness of Upper Devonian sequence in the Syv'yu River section is about 200 m. The sequence is subdivided into the Kedzydshor, Vorota, Shar'yu and Domanicoid formations, and the first three of these formations were earlier described in the Shar'yu River section (Chernyshev Ridge; Tsyganko et al. 1985, see also Yudina 1989). It should be noted that in contrary to previous studies (Tsyganko 1994), the dark-gray organic-rich limestones that were considered as the upper part of Kedzydshor Formation are now included in the Vorota Formation because of their color and predominantly pelagic faunas (Savage and Yudina 1999). Moreover, the upper limit of the Vorota Formation is drawn at the top of the uppermost dark-colored, predominantly shaly beds included earlier in the Shar'yu Formation. Thus, the Vorota Formation in the proposed lithostratigraphic scheme corresponds to a single pelagic sedimentation phase characterized by stagnant conditions within a stagnant relatively deep-water intra-shelf basin. The fourth formation was named by Savage and Yudina (1999) the Domanicoid Formation because it was not distinguished as a separate unit during the large scale geological mapping, and is therefore shown on the latest geological maps of the Subpolar Urals as part of the Famennian.

The Kedzydshor Formation is about 15 m thick and consists of silty clays, siliceous dark-gray silty limestones, and light-gray and yellow clays. The limestones, often bioturbated, contain brachiopods, gastropods, ostracods, crinoids, trilobites, sponge spicules, and scarce conodonts. Traditionally it is considered as a basal transgressive part of Frasnian Stage (Pershina et al. 1971), but the Middle–Upper Devonian boundary is identified (see Ziegler and Sandberg 1990) in the section near the base of the overlying Vorota Formation at the lowest appearance of *Ancyrodella pristina* (see Yudina 1994).

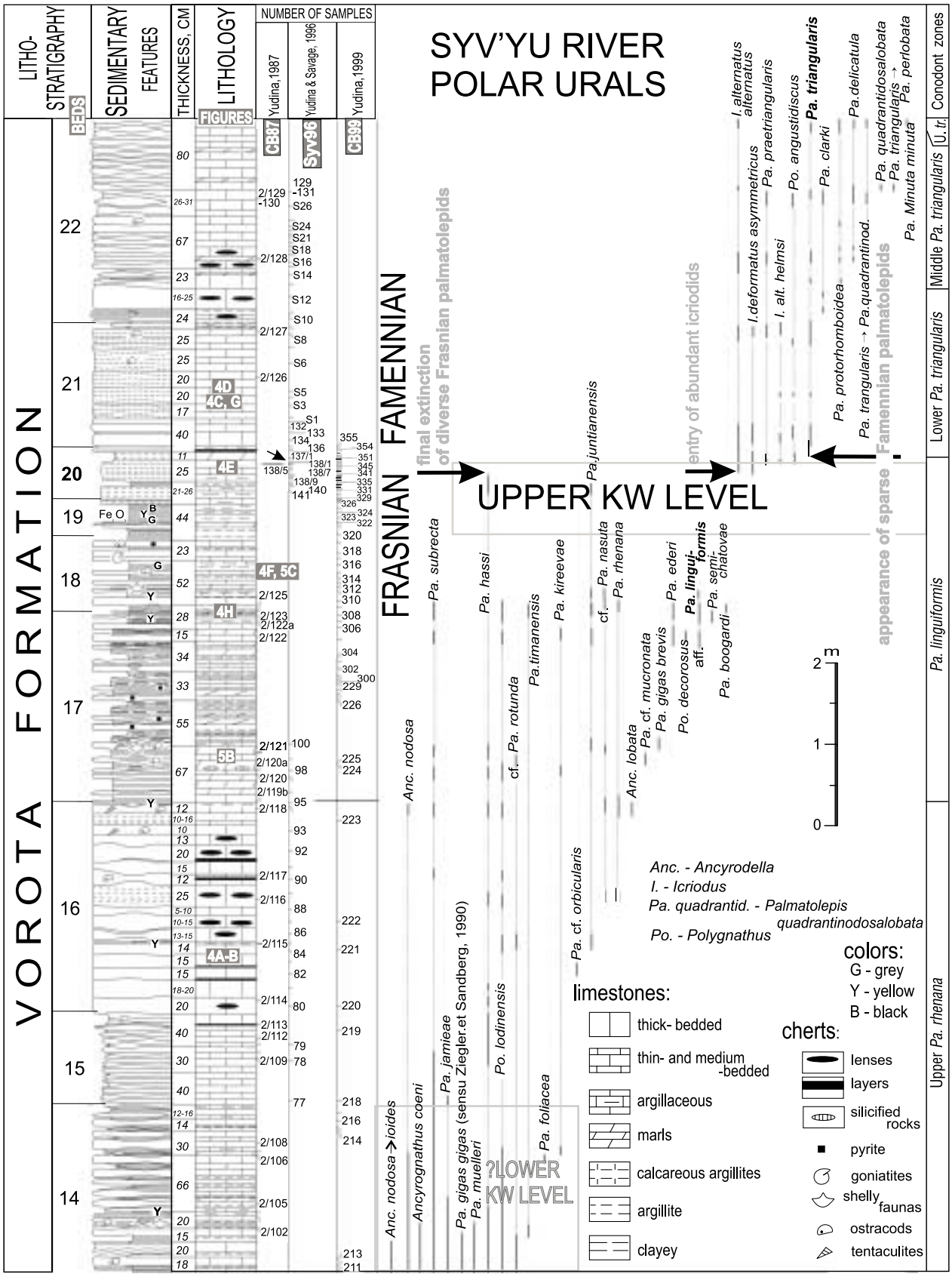

Fig. 4. Upper Frasnian and lower Famennian lithologic column of the Syv'yu River section (upper Vorota Fm.), sampling pattern and conodont succession across the F–F boundary, with emphasis on principal biotic events and alleged Kellwasser levels (see also Figs. 7, 8); figures in the lithological column refer to microfacies photos (Figs. 5, 6).

The Vorota Formation is about 45 m in thickness, and is comprised of three units. The lowest unit (Unit I, 8.2 m thick) consists of black organic-rich and pyrite-rich thin bedded, often laminated, siliceous limestones, argillites, and siliceous shales with thin chert interlayers. The rocks contain tentaculites, radiolarians, goniatites, orthocone cephalopods, bivalves, ostracods, brachiopods, and conodonts. The middle unit (Unit II) consists mostly of gray to dark-gray thin and thick-bedded limestones with interbeds of argillaceous limestones, thin interlayers of brownish-black organic-rich shales, and yellow to yellow-gray clays. Very often the limestones contain black chert nodules and thin lens-like interbeds. In the unit, there are some interbeds composed of finely intercalated shales and nodular limestones. Faunas comprise tentaculites, styliolines, radiolarians(?), thin-shelled brachiopods, ostracods, and conodonts. At the top of the unit, about 14.5 m thick, yellow and gray calcareous clays, and gray to dark-gray marls are present. The upper unit (Unit III), ca. 22 m thick, includes dark-gray to black organic- and pyrite-rich argillaceous and siliceous limestones, often with chert nodules and thin lens-like interbeds, and marly and siliceous marly shales (see below). The faunas in this unit are represented by sponge spicules, radiolarians, scarce thin-shelled brachiopods assigned to *Orbiculoidea*, scolecodonts, ostracods, and conodonts. The base of the Vorota Formation is of earliest Frasnian age, and the top is of early Famennian age (see Fig. 4).

The Shar'yu Formation, early to middle Famennian in age, is about 123 m thick and is composed predominantly of gray to dark-gray, thin- to thick-bedded limestones, marls and marly shales. In the upper part, thick (to 0.6 m) conglomerate-like limestone interbeds occur. Faunas include very scarce, thin-shelled brachiopods assigned to *Orbiculoidea*, ostracods, and rare conodonts. The Domanicoid Formation is about 23 m thick in the section studied. It consists of rhythmically interbedded dark-gray to black thick-bedded massive siliceous limestones with black chert nodules and lens-like nodular limestones. The limestones contain scarce thin-shelled lingulid brachiopods, ostracods and diverse conodonts. The base of the formation is of middle Famennian age and the top extends into the latest Tournaisian–early Visean. The occasional outcrops of the upper part of this formation are known downstream on the Syv'yu River, and on the Kozhym River where Upper Devonian–Carboniferous boundary beds are exposed (Chermnykh et al. 1988; Nemirovskaya et al. 1992).

Frasnian–Famennian lithologic-faunal succession and biostratigraphy

The lithologic and conodont succession across the F–F boundary in the outcrop 2 on the Syv'yu River (see Figs. 1D, 2) is presented below in terms of following numbered beds of the Vorota Formation (Fig. 4), included in the stratigraphic sequence fully described (beds 1–11 and above 27) in Yudina (1999).

Bed 12: about 1.4 m thick. Light-gray thin to thick bedded siliceous limestones (mudstones, wackstones) with thin (1–2 cm) interbeds of dark-gray to black carbonaceous-marly shales, containing tentaculites, fish scales, trilobites, thin-shelled brachiopods and radiolarians (samples CB87-2/90 to 2/95, Syv96-42 to 43).

Bed 13: 3.4 m thick. Thin-to thick-bedded light-gray limestones, often siliceous with thin (to 5 cm) interbeds of dark-gray to black carbonaceous clayey shales. Limestones contain pyrite, sponge spicules, gastropods, radiolarians, tentaculites, burrows and ostracods (CB87-2/96 to 2/101, Syv96-44 to 76).

Bed 14: 1.6 m thick. Lens-like dark-gray limestones (2–6 cm thick) interbedding with brownish-gray marly shales and marls. Limestones contain brachiopods, ostracods and orthocone cephalopods(?) (CB87-2/102 to 2/108; CB99-211-217).

Bed 15: 1.1 m thick. Gray to dark-gray argillaceous limestones with siliceous limestones lenses (concretions?) to 20 cm thick, containing brachiopods, ostracods and tentaculites (CB87-2/109-2/114; CB99-218, 219; Syv96-77-79).

Bed 16: about 2.5 m thick. Thin to thick-bedded gray limestones with nodules and thin black chert lenses, and rare thin interbeds of yellow clays. Fauna comprises ostracods, tentaculites and palmatolepid-ancyrodellid conodont association (CB87-2/115 to 2/118; Syv96-80-95; CB99-220-223).

Bed 17: 2.04 m thick. Thin lens-like alternation of light-gray limestones, often siliceous, and greenish-gray marls; in the middle part there is an interbed of yellow calcareous clay with small pyrite concretions. Limestones contain ostracods, tentaculites, small brachiopods and exclusively palmatolepid conodonts (CB87-2/119b-to 2/122; Syv96-96-100; CB99-224-305).

Bed 18: 1.03 m thick. Yellow calcareous clays and dark-gray argillites with interbeds of light-gray argillaceous limestones and marls, containing pyrite, brachiopods, ostracods, bivalves, tentaculites and palmatolepid conodonts (including

Fig. 5. Microfacies types of the uppermost Frasnian (**A**–**B**, **F**–**G**) and basal Famennian (**C**–**E**) limestones, Syv'yu River section. **A**, **B**. Homoctenid-radiolarian peloidal packstone; sample Syv96-83. **C**. Bivalve shell (?*Buchiola*) in radiolarian-spiculite peloidal packstone; sample Syv96-S3. **D**. Rock-forming problematic rosette-like calcite aggregates (?neomorphozed radiolarians) in slightly stylolaminited packstone; sample Syv96-S5. **E**. Strongly pressure-welded mudstone of the Upper KW level; sample CB99-340. **F**. Marginally aggraded brachiopod wackestone, marked by coarse neospar of homogenous micrite matrix (N); sample CB99-313; **G**. Diagenetic ribbon lamination within the peloidal radiolarian packstone (R; see close-up in C), showing largely neomorphozed (N) and stylolaminated (S) bands; sample Syv96-S3. **H**. Silicified (S) parting of sponge-bearing wackestone with phosphatic(?) concretionary aggregates (P); sample CB99-308. →

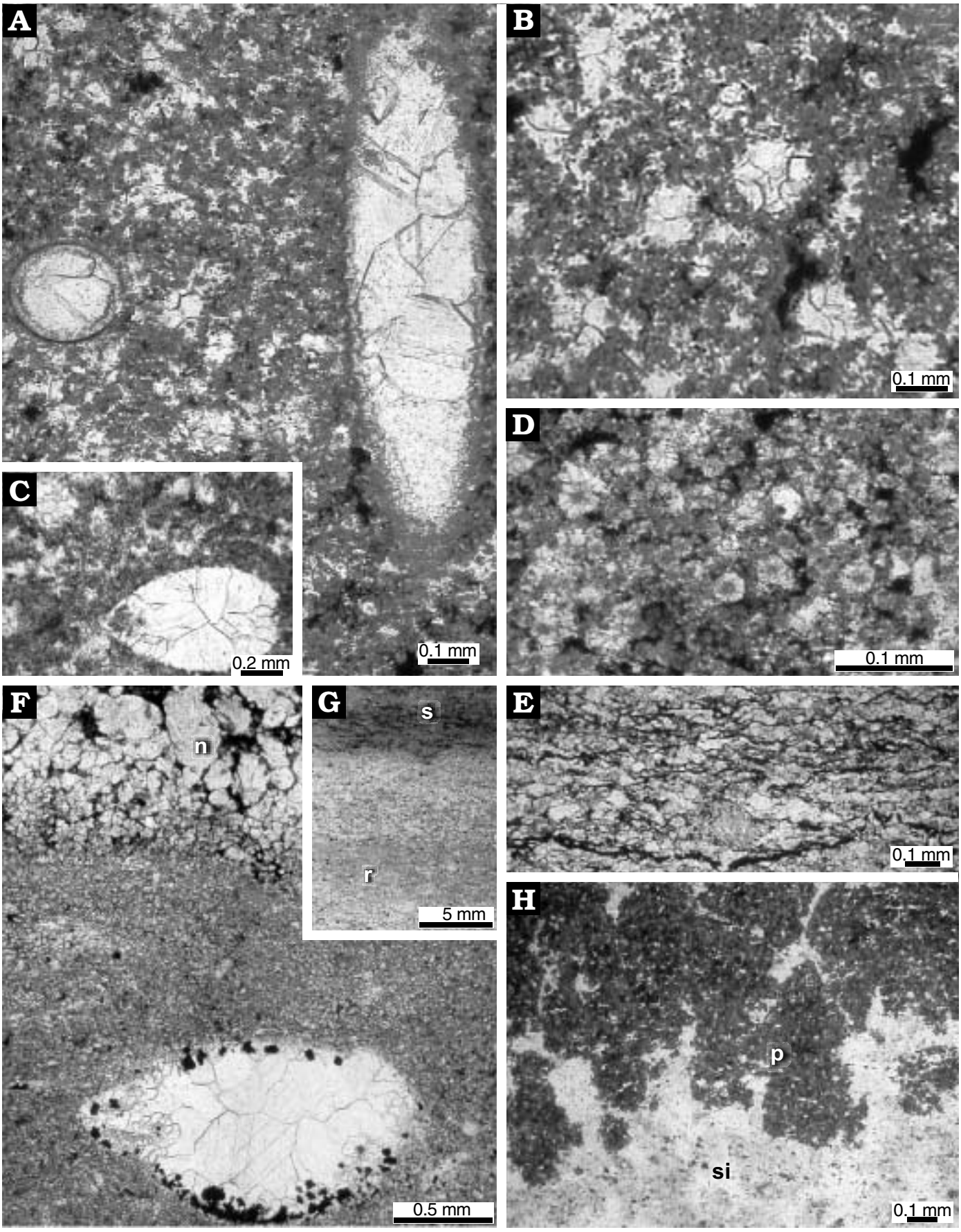
A
0.1 mm
B
0.1 mm
C
0.2 mm
D
0.1 mm
F
n
0.5 mm
G
s
r
5 mm
E
0.1 mm
H
p
si
0.1 mm

abundant *Palmatolepis linguiformis*); in the lower part, argillites contain apparently reworked rounded conodonts of the species *Pa. semichatovae* and pyritized tentaculites; in the upper part the species *Pa. praetriangularis* first appear (CB87-2/123 to 2/125; CB99-224-305).

Bed 19: 0.44 m thick. Clays, gray in the lower part, yellow and black in the upper part. In the middle part of the bed there are thin marl and limestone interbeds. In the upper part clays are rich in iron hydrooxigen (CB99-320-325).

Bed 20: about 0.7 m thick. Thin-bedded black argillaceous limestones and calcareous argillites containing pyritized sponge spicules, rare styliolines and poor conodonts. In the lower part of the key bed Frasnian-type palmatolepids include *Pa. juntianensis* and *Pa. hassi*; in the middle part – icriodontids and polygnathids (*Icriodus deformatus asymmetricus*, *I. alternatus alternatus* and *Po. angustidiscus*), and in the upper part – *Pa. praetriangularis* and *Pa. triangularis*. At the top of the bed there is a 3 cm thick layer of black chert (Syv96-141 to 137/1; CB99-326-354).

Bed 21: 1.5–1.6 m thick. Thin- to thick-bedded dark-gray to black limestones, often siliceous, containing phosphatic(?) brachiopods and conodonts representing palmatolepid-icriodontid-polygnathid biofacies (CB87-2/126 to 2/127; Syv96-136-132, Syv96-S-1 to 8; CB99-355).

Bed 22: 2.5 m thick. Thin-bedded (platy) dark-gray limestones, rich in pyrite, with rare nodules and thin layers of black chert in the lower part; faunas comprise scarce thin-shelled brachiopods, scolecodonts, ostracods, styliolines and almost exclusively palmatolepid conodonts (CB87-2/128 to 2/131; Syv96-S9 to 26, Syv96-131).

Bed 23: about 1.4 m thick. Dark-gray calcareous argillites with rare thin (4–15 cm) interbeds of dark-gray limestones and nodular limestones (1.5–2 cm) containing ostracods and conodonts; in the 0.5 m above of the base there is a thin layer of yellow calcareous clays (CB87-2/132 to 2/134)

Bed 24: about 3.0 m thick. Dark-gray thin platy argillaceous limestones with rare black chert interbeds (to 1.5 cm thick) and dark-gray limestones (3–11 cm), containing scarce ostracods (CB87-2/135 to 2/139).

Bed 25: about 2.2 m thick. Dark-gray thin platy siliceous marls with interbeds composed of large dark-gray limestones lenses (concretions?) containing ostracods only (CB8702/140 to 2/141).

Bed 26: about 9 m thick. Black siliceous(?)-clayey shales with rare thin (3–22 cm) lenses of dark-gray to black siliceous limestones, and massive limestones (to 25 cm thick) (CB87-2/242 to 2/150).

Bed 27: about 2.2 thick. Dark-gray to black thin-platy siliceous limestones with micritic limestone interbeds (to 10 cm thick), containing rare brachiopods *Orbiculoidea* and conodonts (6 palmatolepid species and *Pelekysgnathus*; CB87-2/151-2/156).

Conodont biostratigraphy.—"Standard" conodont zones according to scheme of Ziegler and Sandberg (1990) are fair easily recognized in the *Palmatolepis*-rich Syv'yu River succession.

The Lower *Pa. rhenana* Zone is recognized in the middle part of the Vorota formation (beds 12, 13) on the abundant occurrence of *Pa. semichatovae*, but the index species of the zone, *Pa. nasuta*, was identified higher in the middle part of the bed 13. The Upper *Pa. rhenana* Zone is distinguished on the occurrence of *Pa. subrecta* in the middle part of the Vorota Formation (the upper part of bed 13 to bed 16). Beginning from the bed 16 *Ancyrodella lobata*, *Pa. juntianensis* and *Pa. rhenana* occur. Thus, in the section described the index species of the zone occurs higher. *Pa. gyrata* is known from the Lyayol' Formation (Unit IV) in the South Timan in the part of the sequence that is correlated with Montagne Noire Zones 11–12 (Kuzmin and Melnikova 1991; Klapper et al. 1996).

The *Pa. linguiformis* Zone is recognized in the beds 17–20 by the first occurrence of *Pa. linguiformis*. In the uppermost part of the zone, *Pa. praetriangularis*, icriodontids and polygnathids appear. The lower limit of the *Pa. triangularis* Zone (and the base of Famennian) is defined by the first appearance of *Pa. triangularis*, and the upper limit is defined by the first occurrence of *Pa. delicatula platys*. In the Syv'yu section, the zone is recognized in the upper part of the Vorota Formation (beds 20–21) on the first occurrence of *Pa. triangularis* in sample Syv96-138/1 (see Fig. 4). The boundary between the Middle and Upper *Pa. triangularis* zones has not been properly recognized yet, thought it probably lies somewhere within bed 22. A large number of morphotypes of *Palmatolepis* species in the upper part of the interval may indicate the Upper *Pa. triangularis* Zone. Likewise, the *Pa. crepida* Zone has not been subdivided, but in the bed 24 there were found species typical of this zone. The Upper *Pa. crepida* to *Pa. rhomboidea* zones are poorly characterized by conodonts. The Upper *Pa. crepida* Zone only is reliably documented on the occurrence of *Pa. glabra prima* in the uppermost part of the Vorota Formation (beds 25–27) and in the lowermost part of Shar'yu Formation (bed 28).

Microfacies review

Limestone microfacies of the middle and upper parts of the Vorota Formation are not very differentiated (Figs. 5, 6). Light-gray bed 13 represents mainly lithistid sponge-mud varieties (Fig. 6A; see also Vishnevskaya et al. 2002), characterized by clotted to minipeloidal fabrics of the micritic matrix. Irregular, dense micrite linings due to microbial activity are sporadically observed as well. Burrows, up to 3 mm in diameter, and smooth ostracod valves are frequent, but also abundant homoctenids (and rarely entomozoids and radiolarians?) occur in some beds.

Darker, marly, pyrite-rich lithologies of beds 14 and 15 reveal more diverse biotic content, including homoctenids, entomozoids, conodonts and/or lingulids, as well as shelly faunas (mostly thin-valved bivalves) and burrowers. Limestone interbeds exhibit sparry-peloidal fabrics, partly due to extensive neomorphism. The diagenetic effects, that have finally led to coarse-sparry, marble-like patches and intercalations (Fig.

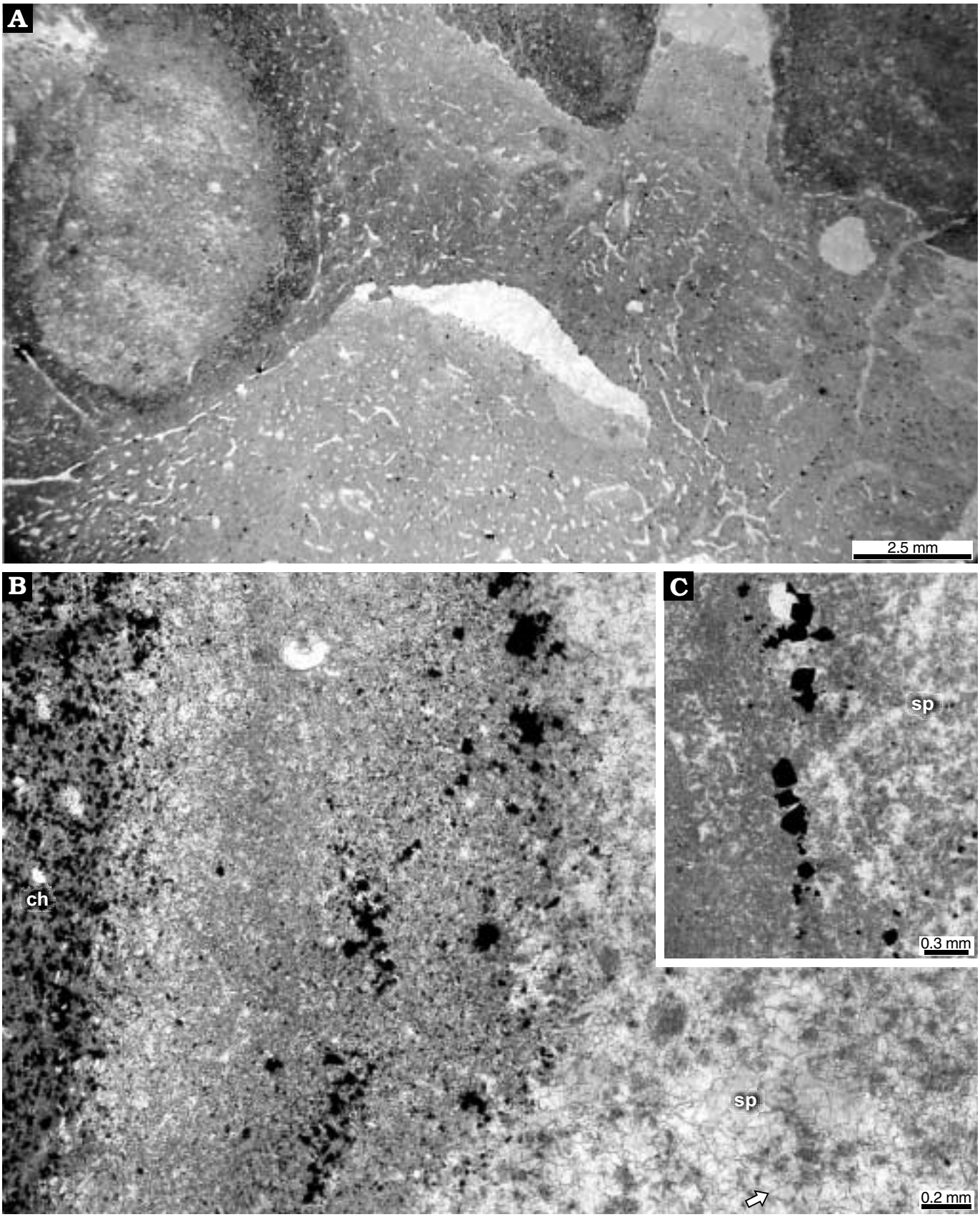

Fig. 6. Various upper Frasnian spongiolitic microfacies, Syv'yu River section. **A**. Sponge boundstone(?); note large growth cavities, and complex and diverse, peloidal to bioclastic geopetal fill up, as well as preserved spicular network; sample Syv96-58. **B**, **C**. Sponge relics (Sp) distinguished by a variety of grumeous fabric, pyrite-rich marginal rims, and partly chertified interstitial mudstone matrix (Ch); samples CB99-224 (**B**) and CB99-314 (**C**).

5F), are frequently observed in several intervals in the organic-rich succession. Also pressure-welded (stylolaminite) bands are common, resulting in crudely laminated to ribbon-like appearance particularly well developed in the F–F transition limestone beds (Fig. 5G).

Gray cherty limestones (bed 16) are characterized by rock-forming calcified radiolarians in peloidal-micritic burrowed matrix; in addition, benthic ostracods, homoctenids, bivalves, and entomozoids are found (Fig. 5A, B), especially abundant in shaly partings. Succeeding rhythmic succession of bed 17 and 18 is more differentiated in microfacies (Figs. 5F and 6B, C), that varies from burrowed pyrite-rich dense mudstones with poorly-preserved sponge relics to irregularly laminated wackestones, bearing diminutive shelly faunas, both brachiopods and bivalves, or homoctenids (also styliolinids?) and/or entomozoids. Silicified parts show large-scale reversals to calcite in places.

The F–F passage (black-colored bed 20) records a return of radiolarian microfacies, but characterized by overall impoverished biotas limited to sponge spicules (abundant in the bottom part) and ostracods; shelly (?bivalve) and burrowing faunas are found only in the basal sample CB99-328. More numerous shelly remains (chiefly bivalves up to 1 cm in size; Fig. 5C) re-appear ca. 0.5 m above the F–F boundary, and this mostly radiolarian-rich, locally burrowed microfacies continues up to bed 21. The common stylolaminite interbeds are distinctly fossil-impoverished (Fig. 5D, E), but may contain very abundant spheres resembling problematic *Palaeomicrodium* algal aggregates (rather peculiarly neomorphozed radiolarians or leiosphere fills). A single crinoid ossicle is found in this interval.

In summary, the deep-water muddy and invariably low-energy environments were populated by varied sponge biota, soft-bodied bioturbators and minute shelly benthos (like the bivalve *Buchiola*; Grimm 1998). Far more abundant pelagic biotas include either calcareous (homoctenid-entomozoid) or calcareous-siliceous (with radiolarians) microfaunas but were rapidly predominated by prolific radiolarian zooplankton just below the F–F boundary. Within the opal-rich calcareous sediments, the silica was extensively redistributed during diagenesis. The common grumous, clotted and/or (mini)peloidal carbonate muds were at least partly produced microbially during decomposition of soft tissue of the radiolarians and sponges, as described from Carboniferous cephalopod and mud-bank limestones by Warnke (1997) and Devuyst and Lees (2001; see also Upper Devonian examples in Préat et al. 1998; Boulvain 2001; Racki et al. 2002).

Geochemistry

Only selected trace element (mostly discussed in Racki et al. 2002) and isotopic guide data from the section studied were used to test for various Earth-bound environmental factors which might have acted in the Timan-Pechora Basin during the KW Crisis timespan (see Figs. 7, 8). Substantial Ir evidence of an extraterrestrial impact was not discovered in the Urals succession (contents below 5 ppb in all samples; see Appendix 2). Many well-known geochemical proxies could not be used because several key elemental concentrations (e.g., Mo, Cd, Th) were too often below the detection limit of analytical methods. For those elements (e.g., for U, Cr), half of the detection limit values were taken into consideration in such sporadic cases.

Trace elements.—From many tested palaeo-oxygenation indices V/(V+Ni) and U/Al ratios were chosen as a reliable proxy, with thresholds for the oxic/dysoxic, dysoxic/anoxic and anoxic/euxinic boundaries adopted herein from Bellanca et al. (1998) and Morford and Emerson (1999: fig. 4; see also Yarincik et al. 2000). Barium, SiO_2 and P_2O_5, were jointly used as the biological productivity record. Measured concentrations of SiO_2, P_2O_5 and Ba were normalized according to Schmitz et al. (1997), i.e., recalculated to the Al_2O_3 content of average continental crust (15%) for Ba and P_2O_5 (e.g., Ba* = Ba/[Al_2O_3 × 15%]), whilst the SiO_2*-excess values represent the total SiO_2 content from which an assumed average SiO_2 content of the aluminosilicate fraction (45%) has been subtracted. Zr/Al_2O_3 ratio was considered to reflect volcanic signals in the context of concurrent F–F tectono-magmatic activation in the Ural Ocean (Nikishin et al. 1996; Veimarn et al. 1997; Kravchinsky et al. 2002). Because hydrothermal deposits have Al/(Al + Fe + Mn) values less than 0.35 and Fe/Ti ratios higher than 20 (Boström 1983) these relations were employed as crude proxies of hydrothermal supply. Average Zr/Al_20_3 and Al/(Al + Fe + Mn) backgound ratios in limestones (see Fig. 7) are calculated from table 1 in Wedepohl (1970).

The above geochemical markers show largely stable values in the studied part of the upper Frasnian succession, but are followed by more or less distinct anomalous levels around the F–F boundary. The excursions start typically ca. 0.7 m below the F–F boundary, within the bottom part of the bed 21, and continue above this key boundary. This noteworthy pattern is especially well manifested for Zr/Al_2O_3, V/(V+Ni), Fe/Ti (not shown), Ba* and SiO_2* curves, but somewhat more obscured for the U/Al ratio and P contents (Fig. 7), as well as for example, Ti/Al ratios regarded as a tracer of basaltic volcanogenic source. In particular, the reconstructed oxygen levels are more or less firmly supported by other signatures (V/Cr, Co/Ni and Al-normalized contents of chalcophiles). The levels of TOC in the key carbonate bed 21 are distinctly higher (TOC between 0.77 and 1.69%, carbonate content between 95.82 and 85.84%, respectively) than in marly deposits of the bed 10 (sample CB99-322: TOC 1.22%, carbonate content 39.43%).

A part of the geochemical evolutions was certainly controlled by terrigenous input, as it is revealed by strong correlation between Al and Zr and V contents (correlation coefficient r = 0.98 and 0.88, respectively). This is not the case for palaeoproductivity tracers (r varies between –0.18 for Si to –0.43 for Ba) or for Fe and Mn (r = 0.40). Thus, despite possibly highly varying terrigenous input in the tectonically active palaeogeographic setting and diagenetic bias in the or-

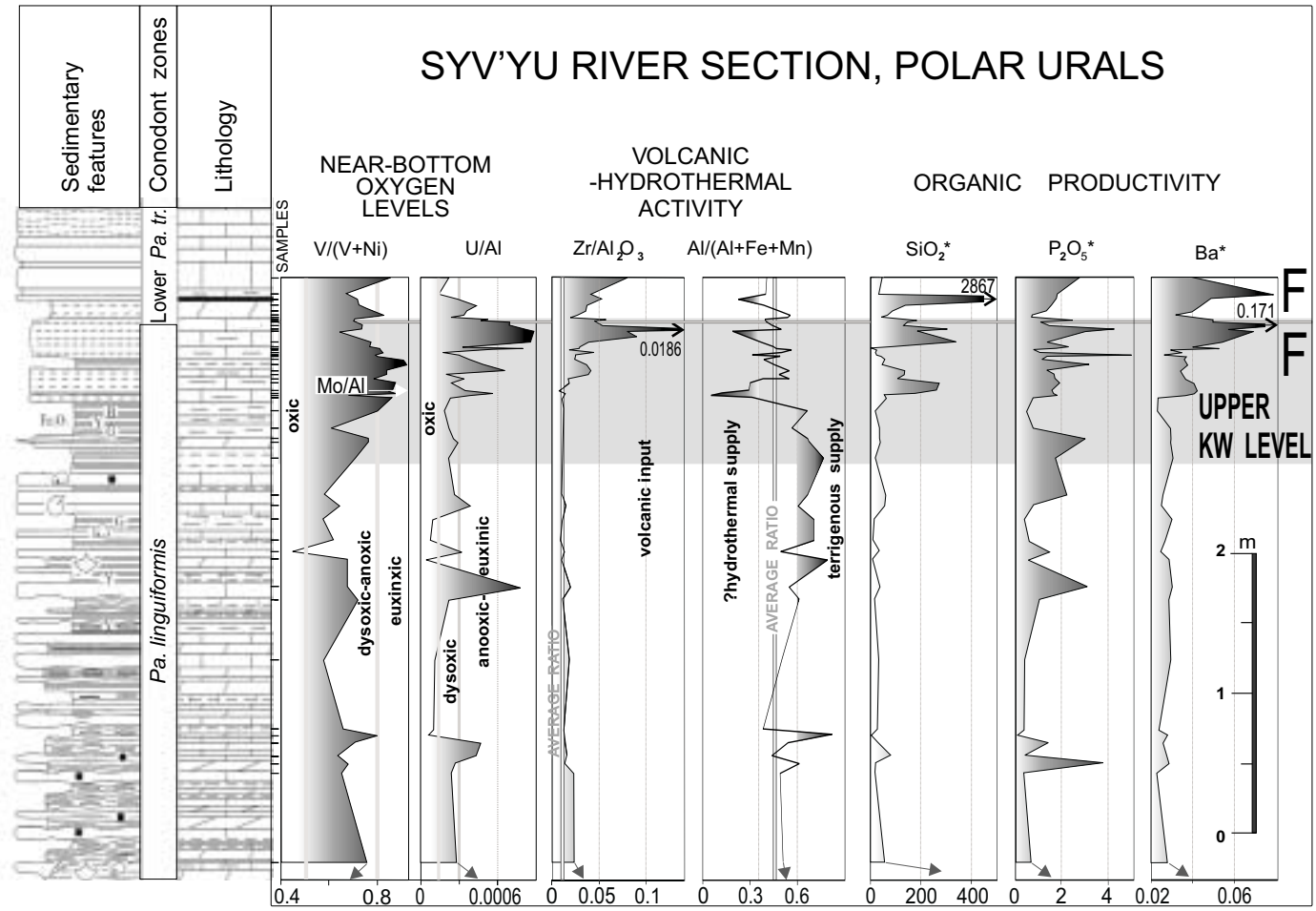

Fig. 7. Trace element environmental proxies for the F–F transition in the Syv'yu River section. Bio-productivity tracers* are normalized according to Schmitz et al. (1997). Downward arrowed trends are based on the single sample CB99-222, located 2.15 m below; recognized Mo/Al enrichment, indicative of anoxic-sulfidic deposition, is shown as well. For explanations see Fig. 4.

ganic-rich deposits, the signatures still monitor major environmental characters and oceanographic signals in the offshore setting (see also Table 1). In this context, it is not surprising that the above elemental anomalies are far more marked in the mostly calcareous beds 20–21 (Al_2O_3 contents below 1%), encompassing the F–F passage, than in the underlying iron-rich clays (bed 19).

Compiling the geochemical and ecological data, the Upper KW Event in the Uralian succession was apparently manifested by progressive near-bottom anoxia toward euxinic regimes and increased bioproductivity, culminating in the thin chert horizon that occurs 11 cm above the F–F boundary (Savage and Yudina 1999: 372). Nevertheless, a high amount of opaline SiO_2, recorded in biogenic cherts of the Syv'yu succession, reflects certainly a bloom of siliceous biota in moderately eutrophic regimes (see Racki and Cordey 2000), as well as in several other Frasnian (bed 16) and Famennian (bed 22) timespans. Enhanced aeolian input of fine-grained pyroclastic material near the F–F boundary might also be suggested for the silica- and organic-enriched interval marked by elevated Zr/Al ratios, especially in light of the mineralogical composition of quartz-dominated insoluble residua. There are up to 20% of presumably volcanogenic admixtures: Na-feldspars, muscovites and other micas, illite–smectite mixed layer clays, and also amorphous particles (?glass shards) and ?anatase. Volcaniclastic turbidites were not distinguished, however, and these overall low levels and not very significant enrichments (e.g., largely below 10 times for Zr/Al ratios), point to dispersive ash input in normal fine-grained sediments (background volcanism *sensu* Zimmerle 1985). Geochemical proof of presumed hydrothermal activity and ferromanganese mineralisation is less supported. Nevertheless, correlation analysis of the most redox-sensitive Fe-Mn and V-U pairings reveals different Mn behavior in the pre-F–F and F–F passage intervals (Table 1), possibly resulting from increased hydrothermal fluxes in the crisis timespan.

Carbon and oxygen stable isotopes.—The carbon isotope record, although based only on the analysis of micrites, reflects a significant increase in ^{13}C just below the F–F boundary from 0 to 3.5‰, in the supposed Upper KW level. Continuing high ^{13}C values are observed throughout the Lower *Pa. triangularis*

Table 1. Correlation coefficients between Al-normalized redox-sensitive metals for the pre-F–F crisis and F–F crisis intervals of the Syv'yu section, capitalizing on the contrasting behavior of the Fe-Mn and V-U pairings (Mo contents, the most diagnostic for anoxic-sulfidic conditions, were mostly below detection limit, Appendix 2; for discussion see Yarincik et al. 2000).

Interval	Predicted POSITIVE correlation		Predicted NEGATIVE correlation			
(No. of samples)	Mn* and Fe*	V* and U*	Mn* and V*	Mn* and U*	Fe* and V*	Fe* and U*
Inter-KW (17)	**0.72**	**0.62**	–0.13	0.24	0.02	0.31
F–F passage (35)	0.05	**0.60**	**0.85**	**0.64**	0.04	0.03

Zone but values gradually approach the background level (1‰; Joachimski and Buggisch 1996) higher in the sequence.

The isotopic values measured on the intercalated micritic and shaly deposits show some scatter, but only two samples in this interval (from the argillaceous bed 19) show a strong negative "anomaly" (paired with lowered ^{18}O values; Fig. 8). Furthermore, microfacies analysis shows that the micritic matrix bears clear evidence for intense recrystallisation, as well as precipitation of neospar predominantly near the transition into the calcareous shales (see Fig. 5F). This observation suggests that diagenetic processes may have somewhat reset the carbon isotopic signals (see Joachimski et al. 2002). A similar negative bias is detected in 6 pilot samples from an alleged Lower KW level, and only one sample from bed 16 exhibits increased ^{13}C values to 2.88‰ that suggests a second positive excursion in the Upper *Pa. rhenana* Zone. On the other hand, abundance of light carbon variety in single sample from the bed 15 (–3.7‰) might be a signature of methane release through dissociation of gas hydrates (as advocated for the F–F boundary events by Bratton 1999). In summary, the present study confirms the worldwide pattern of carbon isotope record at least for the Upper KW Event, recognized for both inorganic and total organic carbon as well as for individual organic biomarkers (Joachimski et al. 2002). This isotope event is interpreted as a consequence of the increase in bioproductivity and organic carbon burial.

The oxygen isotope record, plotted in Fig. 8, is not correlated with the ^{13}C values (r = 0.24) and is relatively stabilized at –6‰, which confirms a mostly primary origin for the isotopic compositions (this coherence equals 0.89 for 9 omitted samples). The significant short-lived negative ^{18}O excursion down to –10.4‰ is restricted to the 20 cm thick interval just above the F–F boundary, but its primary (e.g., a warming episode) vs. diagenetic meaning remains uncertain. Consequently, there is no ^{18}O evidence in the Timan-Pechora Basin for an oceanic cooling (see below), as shown by oxygen isotopic results derived from biogenic phosphates by Joachimski and Buggisch (2000). The Devonian carbonate isotopic record is seen recently as overall indecisive in the palaeoclimatic context, even if useful in tracing of Palaeozoic glaciations (e.g., in the Silurian and Carboniferous; Azmy et al. 1998; Saltzman 2002).

Mechanisms related to Frasnian–Famennian events in the Timan-Pechora Basin

The Syv'yu section is the northernmost F–F succession studied in combined, event-stratigraphic categories. Although located below 30°N, this north-eastern Laurussian shelf slope was far more exposed to open-oceanic influences than, for example, the corresponding North African domain of the southern (Gondwanan) hemisphere. This is revealed by the direct association of Pechora-Urals reefs and upwelling, highlighted by Kiessling et al. (1999: 1564; but see House et al. 2000). The offshore deep-water environmental aspects are well defined by a lack of any shallow-water, especially reef-derived debris supply, and abundance of planktic, both calcareous and silicic biotas. The oceanographic specificity is perfectly manifested by biosiliceous, organic-rich deposition of middle Frasnian Domanic facies (e.g., Afanasjeva 2000; House et al. 2000). On the other hand, poorly-known sponge-micriobial(?) mud buildups might in fact represent a Frasnian praecursor of the Waulsortian facies. A comparable sponge and iron-bacteria consortium occurs in lower hypoxic parts of Belgian late Frasnian carbonate mounds (Boulvain 2001).

A good accordance of the recognized events over the Pechora-Urals domain with the Euramerican T–R cylicity of Johnson et al. (1985) and Sandberg et al. (1988) is discussed by Veimarn et al. (1997) and House et al. (2000). The Lower KW horizon is tentatively presumed for thin-bedded dark-gray limestones interbedding with brownish-gray marly shales and clayey marls (bed 14) in the Upper *Pa. rhenana* Zone (Fig. 4), but this needs more detailed geochemical (especially $^{13}C_{org}$) and ecological study because of possible benthos presence in some layers. Inter-KW timespan is marked by varying carbonate-clay deposition in the typically dysaerobic and low-productivity setting, interrupted by biosiliceous and/or anoxic episodes related to fertilization pulses.

In contrast to the southern Timan basin, an onset of the anoxic Upper KW Event may be recognized in the *Pa. linguiformis* Zone in the fossil-impoverished clay-rich unit 19 (see also black shaly interval $34^{b\text{-}v}$ in the Shar'yu River section; Yudina 1989). Carbon isotopic shift is observed evidently in the transition from the topmost black portion of this unit to a succession of thinly bedded dark-gray to black deposits, often siliceous (ca. 2.2 m thick; beds 20–21). A prominent diagenetic overprint is obvious for the anoxia onset, especially for the isotopic record in the underlying argillaceous interval (Fig. 8), and probably obscured also the metal signatures under changing redox conditions (see e.g., Yarincik et al. 2000). The F–F boundary level is located ca. 0.7 m above the base of the limestone unit, without remarkable lithological change. However, this critical interval is marked by significant biotic perturbations, manifested in near-disappearance of benthic faunas (only silicisponges and inarticulates?) and turnover in pelagic biotas, i.e., replacement of palmatolepid conodont biofacies by

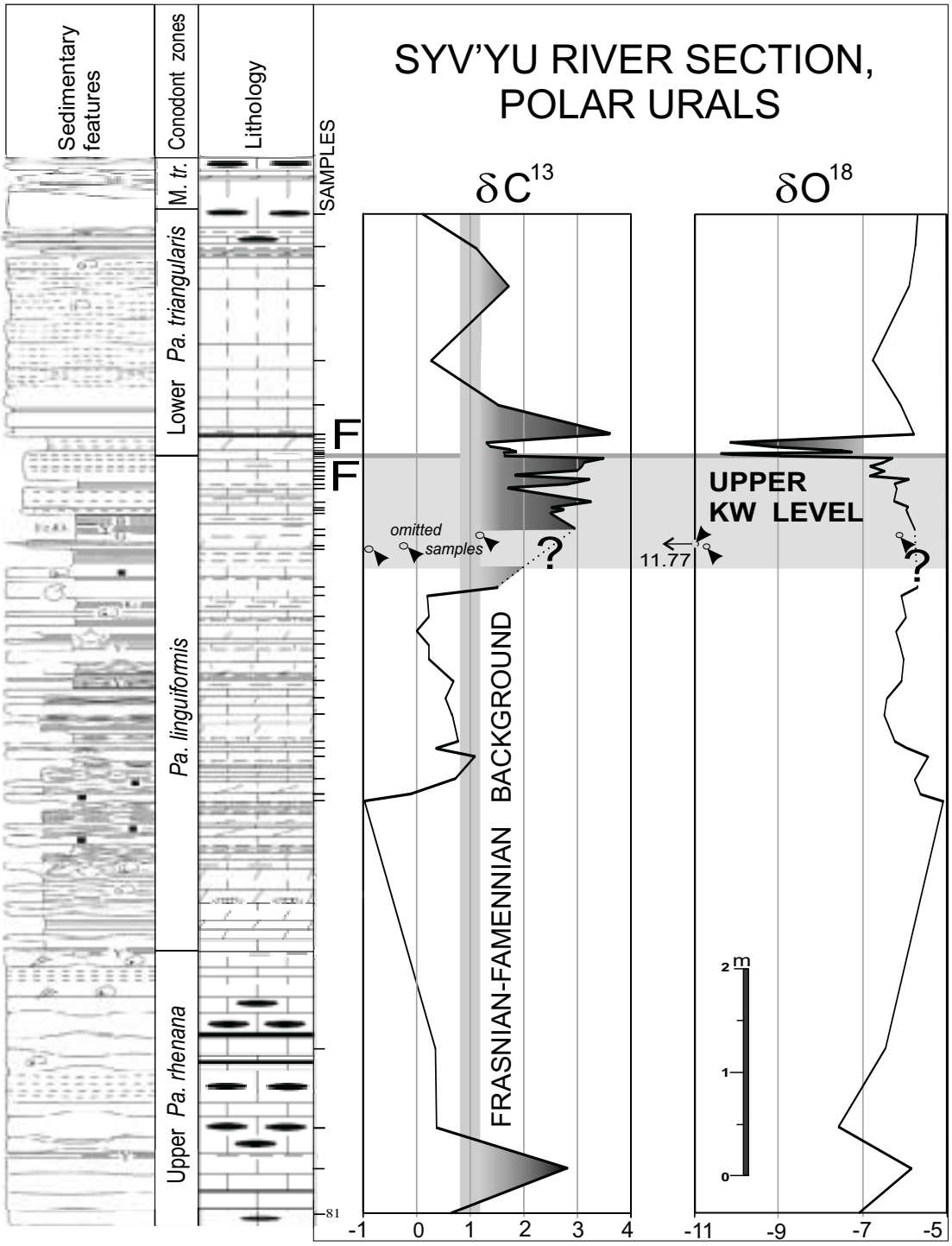

Fig. 8. Stable isotope geochemistry for the Upper Frasnian and lower Famennian in the Syv'yu River section, F–F background values taken from Joachimski and Buggisch (1996: fig. 1); for explanations see Fig. 4.

palmatolepid-icriodontid-polygnathid biofacies (Savage and Yudina 1999: 372) and explosive flourishing of radiolarians.

The ecological shift is paired with trace element anomalies, especially with rapid positive excursion of productivity proxies, and a "heavy carbon" event. These signatures reflect an oceanographic turning point: an expansion of anoxic and high productivity regimes, probably at least partly mediated by a variety of volcanic-hydrothermal phenomena (as modelled for the Mesozoic oceanic anoxia by Jones and Jenkyns 2001). For example, even diluted volcaniclastic input might caused eutrophic conditions due to very high fertilization potential of newly erupted volcanic ash (see Frogner et al. 2001). In addition, silicic exhalative volcanism in zones of reactivated deep faults might control siliceous biota blooms in shelf seas (e.g.,

Maksimova 1979; Afanasjeva 2000; Racki and Cordey 2000). This is in agreement with the F–F biosiliceous acme in many regions of the World (see summary in Racki 1999; also Vishnevskaya et al. 2002). On the other hand, if increased Zr/Al and Ti/Al ratios are thought as a signature of enhanced eolian activity in the critical timespan (see Rachold and Brumsack 2001), thus a wind-driven nutrient-rich upwelling could be presumed for this part of Ural Ocean.

Stable oxygen deficiency, induced by maximum highstand of warm saline deep waters on subtropical shelves, are usually postulated for KW events (see e.g., Joachimski and Buggisch 1996, 2000; Hallam and Wignall 1997), but a scenario of "intermittent (seasonal) anoxic events" has recently been advocated (Hudson 2001). Sedimentary record of storm wave reworking, as well as the recognition that benthic colonization was much more widespread than previously believed, suggest that anoxia were not a major control in the mass accumulation of the organic matter present in the Late Devonian black shales (Schieber 2001). Fluctuating redox states and an improving oxygenation during the Upper KW Event are indeed confirmed in many regions (see Racki et al. 2002). However, metal data from the Syv'yu succession suggest fairly uniform, mostly anoxic to euxinic regimes during the F–F interval. For example, a proliferation of epifaunal and/or pseudoplanktic bivalves in recovering Famennian habitats might be still forced by hypoxia (Harries and Little 1999).

A common factor for these potential "Earth-bound only" causes is tectonism which was likely to have been significant in controlling the sea-level fluctuations. A shallowing pulse on the Laurussian shelf seems to be obviously correlated with the latest Frasnian eustatic sea-level fall, and the F–F passage corresponds to a major sequence boundary over the Timan-Pechora carbonate shelf, as discussed by House et al. (2000). This is less clear in the continuous Syv'yu succession, where the Lower *Pa. triangularis* Zone shows more than a 2 m thick stratigraphic record, and accelerated off-shoal lime ooze input and sudden re-establishment of pure calcareous-biosiliceous deposition comprise a conspicuous sedimentary character. This facies change might have been controlled in part by local block uplifts and/or oceanic overturn (see discussion in Racki et al. 2002). In particular, accelerated orogenic activity in the Zilair-Magnitogorsk arc-trench basin of the southern Urals is indicated by flysch deposits at the F–F transition (Veimarn et al. 1997); this collision with the Mugodjarian terrane was accompanied by a phase of compressional deformation of the adjacent Sakmarian back-arc basin (Ziegler 1988: 33; Khain and Seslavinsky 1996: 185). Therefore, intermittent extension gradually abated in the west-dipping Uralian subduction system, and the phase of rapid post-rift compensated subsidence during middle Frasnian to Famennian characterizes the Pechora Plate (Nikishin et al. 1996: 49–51).

Altogether, the region-wide F–F tectonic instability might be a result of global-scale changes in plate interactions, incipient continental break-up and triple junction formation, or episodic mantle plume activity (Nikishin et al. 1996; Wilson and Lyashkevich 1996; Kravchinsky et al. 2002) recorded in distinctive magmatism, rifting, domal basement uplift and specific metallogenesis in the Urals and within the East European and Siberian cratons (see review in Veimarn et al. 1997; Kravchinsky et al. 2002). This is exemplified by submarine basic extrusive-exhalative processes recorded in the black shaly-siliceous strata of the Pay Khoy basin (Yudovich et al. 1998: 62–91, 344–345) (see Fig. 1B), and a general transition from calc-alkaline gabbro-granite intrusives to tonalite-granodiorite batholiths was manifested in Late Devonian Uralian magmatism (Fershtater et al. 1997: fig. 5; see also Khain and Seslavinsky 1996). Also in the SW part of Moscow epeiric sea, the latest Frasnian eruptive volcanism is deduced from a smectite-type clay admixture rich in quartz and albite (Vengerchev 1995).

Overall climatic variation, especially frequently repeated oceanic cooling in the context of expanding biosiliceous deposition (Copper 1998; see also review in Streel et al. 2000), is still enigmatically recorded in the Uralian succession. The introduction of evaporitic facies over the adjoining Timan shelf in the terminal Frasnian is emphasized by House et al. (2000), and overall arid climate evidence is outlined by Dubotalov and Krasnov (2000). Thus, a warming pulse in the north-eastern Laurussian shelf, as supposed by Becker and House (1994), can be further considered.

The Syv'yu deep-shelf succession exhibits surprisingly numerous analogies to the southern Holy Cross Mts., Poland, which represent a more shallow-water rhythmic hemipelagic facies of a localized intrashelf basin (Kowala section; Racki et al. 2002). This is visible in correlative lithological and ecological F–F shifts from clay-rich to calcareous-biosiliceous sedimentation, even if unsteady redox and eutrophication/productivity regimes are probably more characteristic of the Polish basin. Also compatible development of more (Urals) or less (Holy Cross Mts.) distinctive spongiolitic-cherty facies in the early KW Crisis is a notable feature (Vishnevskaya et al. 2002). The similarities probably are related to a comparable depositional influence by synsedimentary faulting and hydrovolcanic activity in these well-separated Laurussian shelf regions, quite different from, for example, that in other south Poland intrashelf basins (Racki et al. 2002), as well as in the carbonate ramp of northern Gondwana (the deep-water F–F stratotype succession at Coumiac, Montagne Noire; Préat et al. 1998)

Conclusions

- The F–F boundary is well biostratigraphically documented in the *Palmatolepis*-rich deposits exposed along the Syv'yu River in the lower slopes of the Subpolar Urals. The thin-bedded calcareous-clayey-siliceous deep-shelf sequence appears to represent continuous Domanic-type deposition throughout the world-wide carbonate crisis, without evidence for a basal Famennian hiatus or large-scale sedimentary perturbation within a regressive setting as shown for the adjacent Timan carbonate shelf (House et

al. 2000). This resembles both the radiolarite and siliceous-argillaceous sequence of Pay Khoy (Veimarn et al. 1997; Yudovich et al. 1998: fig. 2), as well as clay-siliceous and carbonate (nodular limestone) successions of the northernmost Kolyma continent (Gagiev 1985, 1997; Karaulov and Gretschischnikova 1997).

- The northernmost Laurussian sequence reveals a regional record of several more or less known F–F global events, summarized by Sandberg et al. (1988), McGhee (1996), Joachimski et al. (2002) and Racki et al. (2002). This is well visible in icriodontid and radiolarian blooms throughout in the critical interval, as well as by the appearance of organic- and clay-rich KW-type deposits (beds 19–20), and a correlative shift of several geochemical proxies recording hypoxic and high-productivity regimes, perfectly exemplified by positive $^{13}C_{carb}$ excursions of +3.5‰.
- The prolonged environmental stress in the NE-Laurussian shelf habitats is mostly ascribed to increasing oxygen deficiency and/or unbalanced nutrient dynamics in disturbed greenhouse climatic and active synsedimentary tectonic settings. Carbon isotope and ecological signatures do not show any evidence for a decrease in primary productivity that was previously assumed as a consequence of an extraterrestrial impact (see e.g., McGhee 1996; Joachimski et al. 2002). Unsteady eutrophic, and oxygen-deficient ecosystems during the KW Crisis might be assumed, especially when intensified by various tectono-volcanic spasms (see review in Racki and Cordey 2000) in the incipiently closing Ural Ocean. Whether this bloom of primary producers was triggered mostly by accelerated nutrient supply from various upwelling systems or continental runoff remains speculative at this stage of study (e.g., House et al. 2000; Racki et al. 2002). For example, the latter excess nutrients might be tectonically stimulated (see Peterhansel and Pratt 2001) by the developing orogeny in the Uralian belt and along the eastern passive margin of Laurussia.

Acknowledgements

Special acknowledgements are due to journal referees Michael R. House and Krzysztof P. Krajewski for their careful examination and stimulative discussion, and Michael M. Joachimski for helpful comment on the draft. We thank Grażyna Bzowska and Leszek Marynowski for mineralogical and organic geochemical analyses, respectively, and Ewa Teper, Marcin Lewandowski, and Anna Sitek for digital preparation of figures. The study is supported by the State Committee for Scientific Research (KBN grant P04D 024 13 to G. Racki) and Silesian University. Geochemical works were encompassed by IGCP Project No. 386.

References

Afanasjeva, M.S. [Afanas'eva, M.S.] 2000. *Atlas Radiolarii Paleozoâ Russkoj Platformy.* 350 pp. Scientific World, Moskva.

Azmy, K., Veizer, J., Bassett, M.G., and Copper P. 1998. Oxygen and carbon isotopic composition of Silurian brachiopods: implications for coeval seawater and glaciations. *Bulletin of the Geological Society of America* 110: 1499–1512.

Becker, T. and House, M.R. 1994. Kellwasser events and goniatite successions in the Devonian of the Montagne Noire, with comments on possible causations. *Courier Forschungsinstitut Senckenberg* 169: 45–77.

Becker, R.T., House, M.R., Menner, V.V., and Ovnatanova, N.S. 2000. Revision of ammonoid biostratigraphy in the Frasnian (Upper Devonian) of the Southern Timan (Northeast Russian Platform). *Acta Geologica Polonica* 50: 67–97.

Bellanca, A., Claps, M., Erba, E., Masetti, D., Neri, R., Premoli Silva, I., and Venezia, F. 1996. Orbitally induced limestone/marlstone rhythms in the Albian–Cenomanian Cismon section (Venetian region, northern Italy): sedimentology, calcareous and siliceous plankton distribution, elemental and isotope geochemistry. *Palaeogeography, Palaeoclimatology, Palaeoecolology* 126: 227–260.

Boström, K. 1983. Genesis of ferromanganese deposits - diagnostic criteria for recent and old deposits. *In*: P.A. Rona, K. Boström, L. Laubier, and K.L. Smith (eds.), *Hydrothermal Processes at Seafloor Spreading Centers*, 473–489. Plenum Press, New York.

Boulvain, F. 2001. Facies architecture and diagenesis of Belgian Late Frasnian carbonate mounds. *Sedimentary Geology* 145: 269–294.

Chermnykh, V.A. [Čermnyh, V.A.], Kochetkova, N.M. [Kočetkova, N.M.], Pazuhin, V.N., Lipina, O.A., Nemirovskaya, T.I. [Nemirovskaâ, T.I.], and Tkacheva, I.D. [Tkačeva, I.D.] 1988. Devonian–Carboniferous boundary deposits of the Northern and Subpolar Urals [in Russian]. *In*: *Pogranič nye Devonsko–Kammennougolnye otloženiâ Severnogo i Pripolârnogo Urala*, 145–151. Nauka i Tehnika, Minsk.

Copper, P. 1998. Evaluating the Frasnian–Famennian mass extinction: comparing brachiopod faunas. *Acta Palaeontologica Polonica* 43: 137–154.

Deulin Y.V. 1987. Zonal and stage subdivision of the late Devonian deposits of the western slope of Subpolar Urals (the Syv'yu River basin) on conodonts [in Russian]. *In*: N.V. Krucinina (ed.), *Sovremnnoe Znacenie Paleontologii dla Stratigrafii. Tezisy Dokladov XXIV Sessii Vsesoyuznogo Paleontologiceskogo Obŝestva SSSR*, 27–28. Leningrad.

Devuyst, F.X. and Lees, A. 2001. The initiation of Waulsortian buildups in Western Ireland. *Sedimentology* 48: 1121–1148.

Dubotalov, V.N. and Krasnov, V.I. 2000. Evolution of geographic settings of Siberian seas in the Famennian [in Russian]. *Geologiâ i Geofizyka* 41: 239–254.

Fershtater, G.B., Montero, P., Borodina, N.S., Pushkarev, E.V., Smirnov, V.N., and Bea, F. 1997. Uralian magmatism: an overview. *Tectonophysics* 276: 87–102.

Frogner, P., Gíslason, S.R., and Óskarsson, N. 2001. Fertilizing potential of volcanic ash in ocean surface water. *Geology* 29: 487–490.

Gagiev, M.H. 1985. Subdivision and correlation of Frasnian–Famennian boundary deposits (in terms of conodonts), USSR North-East (Fore-Kolyma Uplift). *Courier Forschungsinstitut Senckenberg* 75: 53–64.

Gagiev, M.H. 1997. Sedimentary evolution and sea-level fluctuations in the Devonian of North-east Asia. *Courier Forschungsinstitut Senckenberg* 199: 75–82.

Grimm, M.C. 1998. Systematik und Paläoökologie der Buchiolinae nov. subfam., Cardiolidae, Arcoida, Lamellibranchiata, Devon. *Schweizerische Paläontologischen Abhandlungen* 118: 1–135.

Hallam, A. and Wignall, P.B. 1997. *Mass Extinctions and Their Aftermath*. 320 pp. Oxford University Press, Oxford.

Harries, P.J. and Little, C.T.S. 1999. The early Jurassic (Toarcian) and the Cenomanian–Turonian (Late Cretaceous) mass extinctions: similarities and contrasts. *Palaeogeography, Palaeoclimatology, Palaeoecolology* 154: 39–66.

House, M.R., Menner, V.V., Becker, R.T., Klapper, G., Ovnatanova, N.S., and Kuzmin, V. 2000. Reef episodes, anoxia and sea-level changes in the Frasnian of the southern Timan (NE Russian Platform). *Geological Society Special Publications* 178: 147–176.

Hudson, J.D. 2001. Advances in the study of "black shales": source rocks for bricks and hydrocarbons. *Proceedings, Yorskshire Geological Society* 53: 231–236.

Joachimski, M.M. and Buggisch, W. 1996. The Upper Devonian reef crisis – insights from the carbon isotope record. *Göttinger Arbeiten zur Geologie und Paläontologie, Special Volume* 2: 365–377.

Joachimski, M.M. and Buggisch, W. 2000. The Late Devonian mass extinction - impact or Earth-bound event? Catastrophic Events and Mass Extinctions: Impact and Beyond. *Lunar and Planetary Institute Contribution* 1053: 83–84.

Joachimski, M.M., Pancost, R.D., Freeman, K.H., Ostertag-Henning, C., and Buggisch, W. 2002. Carbon isotope geochemistry of the Frasnian/Famennian transition. *Palaeogeography, Palaeoclimatology, Palaeoecolology* 181: 91–110.

Johnson, J.G., Klapper, G., and Sandberg, C.A. 1985. Devonian eustatic fluctuations in Euramerica. *Bulletin of the Geological Society of America* 96: 567–587.

Jones, C.E. and Jenkyns, H.C. 2001. Seawater strontium isotopes, oceanic anoxic events, and seafloor hydrothermal activity in the Jurassic and Cretaceous. *American Journal of Science* 301: 112–149.

Karaulov, V.B. and Gretschischnikova, I.A. 1997. Devonian eustatic fluctuations in North Eurasia. *Courier Forschungsinstitut Senckenberg* 199: 13–23.

Khain, V.E. and Seslavinsky, K.B. 1996. *Historical Geotectonics. Palaeozoic*. 414 pp. A.A. Balkema, Rotterdam.

Kiessling, W., Flügel, E. and Golonka, J. 1999. Paleoreef maps: evaluation of a comprehensive database on Phanerozoic reefs. *American Association of Petroleum Geologists Bulletin* 83: 1552–1587.

Klapper, G., Kuzmin, A.V. and Ovnatanova, N.S. 1996. Upper Devonian conodonts from the Timan-Pechora region, Russia, and correlation with a Frasnian Composite Standard. *Journal of Paleontology* 70: 131–151.

Kravchinsky, V.A., Konstantinov, K.M., Courtillot, V., Savrasov, J.I., Valet, J.P., Cherniy, S.D., Mishenin, S.G., and Parasotka, B.S. 2002. Palaeomagnetism of East Siberian traps and kimberlites: two new poles and palaeogeographic reconstructions at about 360 and 250 Ma. *Geophysical Journal International* 148: 1–33.

Kuzmin, A.V. and Melnikova, L.I. 1991. Subdivision of the Frasnian and Lower Famennian deposits of the southern part of Khoreiver depression (Timan-Pechora Province) [in Russian]. *Bulletin Moskovskogo Obŝestva Ispytatelej Prirody, Otdel Geologičeskij* 66 (3): 62–72.

Maksimova, S.V. 1979. Biogenic silicates, an indicator of the activity of deep-seated faults. *International Geology Reviews* 21: 869–876.

McGhee, G.R. 1996. *The Late Devonian Mass Extinction. The Frasnian–Famennian Crisis*. 303 pp. Columbia University Press, New York.

Morford, J.L. and Emerson, S. 1999. The geochemistry of redox sensitive trace metals in sediments. *Geochimica et Cosmochimica Acta* 63: 1735–1750.

Nemirovskaya, T.I., Chermnykh, V.A., Kononova, L.I., and Pazukhin, V.N. 1992. Conodonts of the Devonian–Carboniferous boundary section, Kozhym, Polar Urals, Russia. *Annales de la Société géologique de Belgique* 115: 629–647.

Nikishin, A.M., Ziegler, P.A., Stephenson, R.A., Cloetingh, S., Furne, A.V., Fokin, P.A., Ershov, A.V., Bolotov, S.N., Korotaev, M.V., Alekseev, A.S., Gorbachev, V.I., Shipilov, E.V., Lankreijer, A., Bembinova, E.Y., and Shalimov, I.V. 1996. Late Precambrian to Triassic history of the East European Craton—dynamics of sedimentary basin evolution. *Tectonophysics* 268: 23–63.

Novakova, N.G. 1991. Facies peculiarities and stratigraphy of the Upper Devonian deposits in the Kozhym Region [in Russian]. *In*: V.S. Cyganko, V.A. Čermnyh, and L.Z. Aminov (eds.), *Geologiâ Devona Severo-Vostoka Evropejskoj Časti SSSR, Tezisy Dokladov*, 54–55. Institut Geologii Komi Naučnogo Centra, Uralskoe Otdelene Akademii Nauk SSSR, Syktyvkar.

Pershina, A.I. [Peršina, A.I], Tsyganko, V.S. [Cyganko, V.S.], Scherbakov, E.S. [Ŝerbakov, E.S.], and Borintseva, N.A. [Borinceva, N.A.] 1971 *Biostratigrafiâ Silurijskih i Devonskih Otloženij Pecorskogo Urala*. 130 pp. Nauka, Leningrad.

Peterhansel, A. and Pratt, B.R. 2001. Nutrient-triggered bioerosion on a giant carbonate platform masking the postextinction Famennian benthic community. *Geology* 29: 1079–1082.

Préat, A., Mamet, B., and Devleeschouwer, X. 1998. Sédimentologie du stratotype de la limite Frasnien–Famennien (Coumiac, Montagne Noire, France). *Bulletin de la Société géologique de France* 169: 331–342.

Racki, G. 1999. Silica-secreting biota and mass extinctions: survival patterns and processes. *Palaeogeography, Palaeoclimatology, Palaeoecolology* 154: 107–132.

Racki, G. and Cordey, F. 2000. Radiolarian palaeoecology and radiolarites: is the present the key to the past? *Earth-Science Reviews* 52: 83–120.

Racki, G., Racka, M., Matyja, H., and Devleeschouwer, X. 2002. The Frasnian/Famennian boundary interval in the South Polish-Moravian shelf basins: integrated event-stratigraphical approach. *Palaeogeography, Palaeoclimatology, Palaeoecolology* 181: 251–297.

Rachold, V. and Brumsack, H.J. 2001. Inorganic geochemistry of Albian sediments from the Lower Saxony Basin NW Germany: palaeoenvironmental constraints and orbital cycles. *Palaeogeography, Palaeoclimatology, Palaeoecolology* 174: 121–143.

Saltzman, M.R. 2002. Carbon and oxygen isotope stratigraphy of the Lower Mississippian (Kinderhookian–lower Osagean), western United States: implications for seawater chemistry and glaciation. *Bulletin of the Geological Society of America* 114: 96–108.

Sandberg, C.A., Ziegler, W., Dreesen, R., and Butler, J.L. 1988. Late Frasnian mass extinction: conodont event stratigraphy, global changes, and possible causes. *Courier Forschungsinstitut Senckenberg* 102: 263–307.

Savage, N.M. and Yudina, A.B. 1999. Late Devonian Syv'yu River section, Timan-Pechora Basin, Northwestern Russia. *Bolletino della Società Paleontologica Italiana* 37: 361–373.

Savage, N.M. and Yudina, A.B. 2001. Late Devonian (Frasnian) conodonts from the Timan-Pechora Basin, Russia. *Journal of the Czech Geological Society* 46: 287–298.

Schieber, J. 2001. A role for organic petrology in integrated studies of mudrocks: examples from Devonian black shales of the eastern US. *International Journal of Coal Geology* 47: 171–187.

Schindler, E. 1993. Event-stratigraphic markers within the Kellwasser Crisis near the Frasnian/Famennian boundary (Upper Devonian) in Germany. *Palaeogeography, Palaeoclimatology, Palaeoecolology* 104: 115–125.

Schmitz, B., Charisi, S.D., Thompson, E.I., and Speijer, R.P. 1997. Barium, SiO_2 (excess), and P_2O_5 as proxies of biological productivity in the Middle East during the Palaeocene and the latest Palaeocene benthic extinction event. *Terra Nova* 9: 95–99.

Streel M., Caputo M.V., Loboziak S., and Melo J.H.G. 2000. Late Frasnian – Famennian climates based on palynomorph analyses and the question of the Late Devonian glaciations. *Earth-Science Reviews* 52: 121–173.

Tsyganko, V.S. [Cyganko, V.S] 1994. Problems of a regional stratigraphic subdivisions classification [in Russian]. *Komi Naučnij Centr, Uralskoe Otdelenie Akademii Nauk SSSR, Naučnye Doklady* 334: 1–20.

Tsyganko, V.S. [Cyganko, V.S.], Pershina, A.I. [Peršina, A.I], and Yudina, A.B. [Ûdina, A.B.] 1985. To the Devonian stratigraphy of the Chernyshev Ridge [in Russian]. *In*: V.A. Molin and B.I. Guslicer (eds.), Rašclenene i Korrelaciâ Fanerozojskih Otloženij Evropejskogo Severa SSSR. *Institut Geologii Komi Filiâla Akademii Nauk SSSR, Trudy* 54: 17–26.

Veimarn, A.B., Kuzmin, A.V., Kononova, L.I., Baryshev, V.N., and Vorontzova, T.N. 1997. Geological events at the Frasnian/Famennian boundary on the territory of Kazakhstan, Urals and adjacent regions of the Russian Plate. *Courier Forschungsinstitut Senckenberg* 199: 37–50.

Vengerchev, V.S. [Vengerčev, V.S.] 1995. Lithological analysis of Frasnian deposits in the south Kaluga area (borehole UG-1) [in Russian]. *In*: L.N. Klenina (ed.), *Biostratigrafiâ Srednego-Gornogo Paleozoâ Russkoj Platformy i Skladcatyh Oblastej Urala i Tân'-Šanâ*, 180–188. VNIGNI, Moskva.

Vishnevskaya, V., Pisera, A., and Racki, G. 2002. Siliceous biota and the Late Devonian biotic crisis: the Polish reference. *Acta Palaeontologica Polonica* 47: 211–226.

Walliser, O.H. 1996. Global events in the Devonian and Carboniferous. *In*: O.H. Walliser (ed.), *Global Events and Event Stratigraphy in the Phanerozoic*, 225–250. Springer Verlag, Berlin.

Warnke, K. 1997. Microbial carbonate production in a starved basin: the *crenistria* limestone of the Upper Visean German Kulm facies. *Palaeogeography, Palaeoclimatology, Palaeoecolology* 130: 209–225.

Wedepohl, K.H. 1970. Geochemische Daten von sedimentären Karbonaten und Karbonatge-steinen in ihrem faziellen und petrogenetischen Aussagewert. *Verhandlungen der geologischen Bundesanstalt* 4: 692–705.

Wilson, M. and Lyashkevich, Z.M. 1996. Magmatism and the geodynamics of rifting of the Pripyat-Dnieper-Donets Rift, East European Platform. *Tectonophysics* 268: 65–81.

Yarincik, K.M., Murray, R.W., Lyons, T.W., Peterson, L.C., and Haug, G.H. 2000. Oxygenation history of bottom waters in the Cariaco Basin, Venezuela, over the past 578,000 years: results from redox-sensitive metals (Mo, V, Mn, and Fe). *Paleoceanography* 15: 593–604.

Yudin, V.V. [Ûdin, V.V.] 1994. *Orogenez Severa Urala i Paj-Hoâ*. 185 pp. Nauka, Ekaterinburg.

Yudin V.V. [Ûdin, V.V.]and Dedeev, V.A. 1987. Geodinamic model of the Pechora Plate [in Russian]. *In*: N.P. Rosčevskij (ed.), *Komi Naučnyj Centr, Uralskoe Otdelene Akademii Nauk SSSR, Naučnye Doklady* 171: 1–12.

Yudina, A.B. [Ûdina, A.B.] 1989. Conodonts of Frasnian–Famennian Stages boundary deposits of the Chernyshev Ridge and Subpolar Urals [in Russian]. *In*: N.P. Ûškin (ed.), Biostratigrafiâ Fanerozoâ Timano-Pecorskoj Provintsii. *Institut Geologii, Komi Naucnij Centr, Uralskoe Otdelene Rossijskoj Akademii Nauk, Trudy* 73: 32–39.

Yudina, A.B. [Ûdina, A.B.] 1994. Conodonts of Middle–Upper Devonian boundary deposits of the Chernyshev Ridge and Subpolar Urals [in Russian]. *In*: N.P. Ûškin and A.M. Pystin (eds.), *Geologiâ i Mineral'nosyr'evye Resursy Evropeiskogo Severo-vostoka Rossii. Tezisy Vserossijskoj Geologičeskoj Konferencii, Syktyvkar* 1: 45–46.

Yudina, A.B. [Ûdina, A.B.] 1999. *Biostratigrafiâ i Konodonty Verhnego Devona Grâdy Cernyševa i Propolarnogo Urala*. Unpubl. PhD. thesis, Institut Geologii, Komi Naucniy Tsentr, Uralskoje Otdelene Rossijskoj Akademii Nauk, Syktyvkar, Russia.

Yudovich, Yu.E. [Ûdovic, Û.E.], Belyaev, A.A. [Belâev, A.A.], and Ketris, M.P. 1998. *Geohimiâ i Rudogenez Cernyh Slancev Paj-Hoâ.* 363 pp. Nauka, Sankt-Petersburg.

Ziegler, P.A. 1988. Laurussia—the Old Red Continent. *In*: N.J. McMillan, A.F. Embry, A. F., and D.J. Glass (eds.), Devonian of the World. *Canadian Society of Petroleum Geologists Memoir* 14 (1): 15–48.

Ziegler, W. and Sandberg, C.A. 1990. The Late Devonian standard conodont zonation. *Courier Forschungsinstitut Senckenberg* 121: 1–115.

Zimmerle, W. 1985. New aspects on the formation of hydrocarbon source rocks. *Geologische Rundschau* 74: 385–416.

Appendix 1

Chemical data (major elements) of F–F passage deposits from Syv'yu River Section, Subpolar Urals (see Fig. 3); * lower detection limit of the used methods for this sample only.

Sample	Distance	SiO_2	Al_2O_3	TiO_2	Fe_2O_3	MnO	MgO	CaO	Na_2O	K_2O	P_2O_5	LOI	Total
	cm	%	%	%	%	%	%	%	%	%	%	%	%
CB99-222	0	84.71	0.49	0.021	0.37	0.004	0.08	7.37	0.07	0.15	0.12	6.69	100.07
Sv 96-100	215	8.11	1.18	0.046	0.84	0.03	0.6	48.58	0.12	0.27	0.05	38.61	98.44
CB99-226	270	4.89	1.11	0.042	0.83	0.041	0.52	51.86	0.02	0.24	0.03	39.98	99.56
CB99-227	277	31.77	7.04	0.378	3.36	0.028	1.07	28.44	0.15	1.76	1.79	24.38	100.16
CB99-228	284	15.67	1.8	0.073	1.66	0.039	0.8	43.66	0.21	0.36	0.05	34.1	98.41
CB99-229	291	8.78	1.64	0.063	1.01	0.039	0.74	48.4	0.12	0.36	0.16	37.88	99.2
CB99-300	296	53.43	15.79	0.844	2.65	0.011	1.84	8.05	0.05	4.19	0.13	11.82	98.8
CB99-301	301	13.43	2.57	0.093	3.08	0.063	0.81	42.97	0.21	0.45	0.07	35.11	98.87
CB99-305	346	10.94	2.02	0.095	1.47	0.03	0.79	46.07	0.09	0.5	0.06	36.88	98.94
CB99-309	386	32.4	7.66	0.36	3.72	0.032	1.05	25.96	0.04	1.99	0.54	24.99	98.74
CB99-310	394	8.43	1.49	0.067	0.91	0.022	0.65	48.02	0.06	0.35	0.31	38.43	98.73
CB99-312	412	50.74	13.75	0.666	2.77	0.019	1.55	10.96	0.06	3.72	0.54	14.17	98.93
CB99-313	418	11.83	2.18	0.079	1.67	0.019	0.7	45.41	0.09	0.53	0.22	35.84	98.57
CB99-314	425	40.14	11.23	0.536	3.53	0.031	1.43	19.58	0.12	2.96	0.46	20.38	100.39
CB99-316	439	44.56	10.92	0.558	3.44	0.034	1.61	17.08	0.09	2.86	0.29	18.92	100.37
CB99-317	447.5	14.47	2.09	0.082	1.02	0.017	0.73	44.49	0.17	0.47	0.11	35.31	98.95
CB99-318	454.5	13.72	1.95	0.067	0.74	0.017	0.66	44.59	0.08	0.45	0.29	36.19	98.76
CB99-320	479.5	46.99	10.99	0.553	2.55	0.03	1.36	15.36	0.06	2.87	1.29	16.84	98.9
CB99-321	490.5	33.11	5.71	0.249	2.08	0.037	0.85	28.9	0.06	1.45	1.05	25.26	98.75
CB99-322	493	37.06	6.75	0.312	2.53	0.038	0.91	26.04	0.08	1.7	1.37	23.44	100.23
CB99-323	500.5	34.38	6.24	0.306	3.58	0.047	0.85	26.24	0.04	1.56	0.33	25.1	98.67
CB99-325	511.5	40.63	9.66	0.363	3.72	0.032	1.07	17.63	0.08	2.16	0.32	24.62	100.27
CB99-326	520.5	8.09	1.15	0.021	1.9	0.017	0.5	46.61	0.12	0.22	0.06	39.92	98.6
CB99-327	522	6.62	0.98	0.043	13.22	0.018	0.46	39.39	0.06	0.27	0.12	35.66	96.84
CB99-328	523.5	5.22	0.36	0.008	1.98	0.013	0.51	50.35	0.06	0.04	0.04	41.13	99.71
CB99-329	525.5	7.79	0.38	0.008	0.69	0.007	0.47	48.81	0.08	0.01	0.04	40.33	98.61
CB99-330	530.5	11.43	0.54	0.017	0.94	0.013	0.45	47.49	0.06	0.15	0.07	39.25	100.41
CB99-331	532	11.29	1.13	0.042	1.37	0.02	0.44	46.03	0.06	0.25	0.13	38.89	99.66
CB99-332	533.5	13.75	1.14	0.042	0.7	0.017	0.4	44.7	0.05	0.27	0.13	37.95	99.14
CB99-333	535.5	13.15	1.09	0.039	0.87	0.02	0.35	44.77	0.06	0.18	0.1	38.09	98.73
CB99-334	539	7.89	1.26	0.062	0.77	0.02	0.45	47.02	0.07	0.33	0.27	42.17	100.32
CB99-335	542	3.76	0.54	0.013	0.48	0.011	0.47	51.96	0.07	0.08	0.04	42.39	99.8
CB99-336	543.5	2.61	0.44	0.013	0.52	0.009	0.48	52.38	0.07	0.09	0.04	42.8	99.44
CB99-337	545	5.07	1.09	0.046	0.85	0.011	0.56	50.54	0.08	0.25	0.37	41.2	100.06
CB99-338	546.5	2.48	0.55	0.025	0.91	0.011	0.5	51.53	0.08	0.13	0.04	42.54	98.8
CB99-339	548	2.61	0.56	0.017	0.41	0.015	0.48	53.23	0.06	0.08	0.03	42.8	100.3
CB99-340	549	2.3	0.68	0.034	0.38	0.019	0.42	52.89	0.07	0.14	0.08	43.18	100.2
CB99-341	550.5	3.94	0.45	0.008	0.38	0.011	0.45	52.56	0.05	0.11	0.07	42.31	100.34
CB99-342	553.5	5.71	0.22	0.004	0.2	0.007	0.42	52.02	0.05	0.06	0.02	41.56	100.25
CB99-344	561	2.28	0.15	0.004	0.19	0.007	0.47	54.15	0.03	0.02	0.03	43.04	100.37
CB99-345*	563	1.64	0.07	0.006	0.15	0.009	0.5	54.44	0.03	<0.01	0.02	43.12	99.97
CB99-346	566	3.48	0.3	0.008	0.22	0.009	0.49	53.05	0.03	0.26	0.03	42.46	100.34
Sv96-138/1	569	3.42	0.27	0.014	0.26	0.009	0.38	53.45	0.04	0.07	0.02	42.49	100.41
CB99-348	570	3.71	0.24	0.004	0.26	0.011	0.28	53.53	0.03	0.06	0.04	42.28	100.43
CB99-349	571	4.66	0.39	0.019	0.44	0.013	0.26	52.5	0.03	0.14	0.05	41.82	100.32
CB99-350	572.5	5.11	0.87	0.025	0.55	0.015	0.42	49.86	0.05	0.22	0.04	41.36	98.52
CB99-351	574	4.37	0.63	0.026	0.37	0.015	0.42	52.33	0.04	0.17	0.03	42.09	100.49
CB99-352	576.5	4.16	0.48	0.013	0.37	0.015	0.36	52.42	<0.01	0.08	0.04	42.06	99.99
CB99-353	580	5.36	0.43	0.013	0.51	0.013	0.29	52.28	<0.01	0.05	0.04	41.49	100.48
CB99-354	584	66.01	0.34	0.008	0.87	0.007	0.14	17.56	0.06	0.08	0.04	15.07	100.18
CB99-355	587	1.77	0.33	0.008	0.37	0.007	0.53	53.97	0.04	0.06	0.04	42.89	100.02
Sv96-134A	599	1.28	0.21	0.008	0.22	0.011	0.42	55.02	0.05	0.08	0.04	43.05	100.39